SCIENCE

The Surface of the Ice-Age Earth

Quantitative geologic evidence is used to reconstruct
boundary conditions for the climate 18,000 years ago.

CLIMAP Project Members

Over the last few million years the earth's climate has alternated between ice ages and warmer intervals. The cause of these climatic fluctuations is an intriguing and as yet unsolved problem. The difficulty in understanding the cause lies in the complexity and global scope of the climate system, for changes in climate occur over a wide range of time and space scales, and involve interactions within a planetary system that includes the ice sheets, the atmosphere, the surface of the land, and the entire world ocean (1). Thus, any strategy for attacking this problem empirically must be linked to a physical model of the global climate system.

The most detailed and highly developed models of climate are the general circulation models (GCM's) of the atmosphere. General circulation models do not address the problem of long-term climatic change directly. Rather, they attempt to explain in dynamic terms the complex of processes which, by balancing the earth's radiation budgets, maintain a particular climate in equilibrium. On a global grid, the GCM's simulate numerically a time-averaged, three-dimensional atmosphere calculated to be in equilibrium with a stated set of boundary conditions (1, appendix B; 2; 3). These models require that three boundary conditions be specified: the extent and elevation of permanent ice, the global pattern of sea-surface temperature, and the continental geography. In addition, some models require that the albedo (reflectivity) of land surfaces be specified.

In 1971 a consortium of scientists from many institutions (4) was formed to study the history of global climate over the past million years, particularly the elements of that history recorded in deep-sea sediments. This study, known as the CLIMAP project (5), is part of the National Science Foundation's International Decade of Ocean Exploration program. One of CLIMAP's goals is to reconstruct the earth's surface at particular times in the past. These reconstructions can serve as boundary conditions for atmospheric GCM's.

Our scientific strategy can be expressed as a series of climate-simulation experiments. Each experiment has three phases. First, a reconstruction of the average state of climatic boundary conditions is made for a particular, geologically short interval of time. Second, an atmosphere is simulated by a GCM, as was done in the pioneer study by Williams et al. (6). Finally, the accuracy of the simulation is tested against an independent set of geologic data. Substantial scientific benefits are anticipated from each phase. The geological reconstructions, being global in extent and quantitative in nature, should give valuable insights into past climatic and geological processes, quite apart from their role (as boundary conditions) in the second phase. The numerical simulations will serve to evaluate the sensitivity of the GCM to substantial changes in boundary conditions and to elucidate the dynamics of past climates. The final phase will serve as a check on the model's skill.

Our first experiment simulates global climate during an average August at a time when the continental glaciers reached their maximum extent in the last ice age, approximately 18,000 B.P. (years before present). This article presents the results of the geological reconstruction. Subsequent papers (3) will present numerical simulations by the Rand version of the two-level Mintz-Arakawa model (3) and the 11-level atmospheric model of the Geophysical Fluid Dynamics Laboratory (7), and a summary of geological data now available for testing the accuracy of atmospheric simulations. The second experiment will simulate both August and February conditions, 18,000 B.P., using a considerably expanded geological data base for the reconstruction phase. Other experiments will reconstruct different times including the interglacial interval at approximately 120,000 B.P., a time warmer than today.

Task groups identified in (8) reconstructed the four boundary conditions necessary to simulate the 18,000 B.P. atmosphere: (i) the geography of the continents; (ii) the albedo of land and ice surfaces; (iii) the extent and elevation of permanent ice; and (iv) the sea-surface temperature pattern of the world ocean.

The 18,000 B.P. Continents

Geography. Continental geography 18,000 years ago can be approximated by today's configuration with a lowered sea level, the result of the transfer of water from the oceans to continental ice caps. Many authors estimate about –130 m for the last glacial low stand (9). Our estimate, –85 m, was a conservative interpretation based on dated, submerged terraces along continental margins (10) and on undated, wave-cut notches ranging from –75 to –90 m on Caribbean islands (11). The magnitude of possible errors in this estimate will have little effect on the outcome of calcu-

The authors are A. McIntyre, T. C. Moore, B. Andersen, W. Balsam, A. Bé, C. Brunner, J. Cooley, T. Crowley, G. Denton, J. Gardner, K. Geitzenauer, J. D. Hays, W. Hutson, J. Imbrie, G. Irving, T. Kellogg, J. Kennett, N. Kipp, G. Kukla, H. Kukla, J. Lozano, B. Luz, S. Mangion, R. K. Matthews, P. Mayewski, B. Molfino, D. Ninkovich, N. Opdyke, W. Prell, J. Robertson, W. F. Ruddiman, H. Sachs, T. Saito, N. Shackleton, H. Thierstein, and P. Thompson. CLIMAP is a multi-institutional consortium of scientists studying long-term climatic change; its administrative center is Lamont-Doherty Geological Observatory of Columbia University, Palisades, New York 10964.
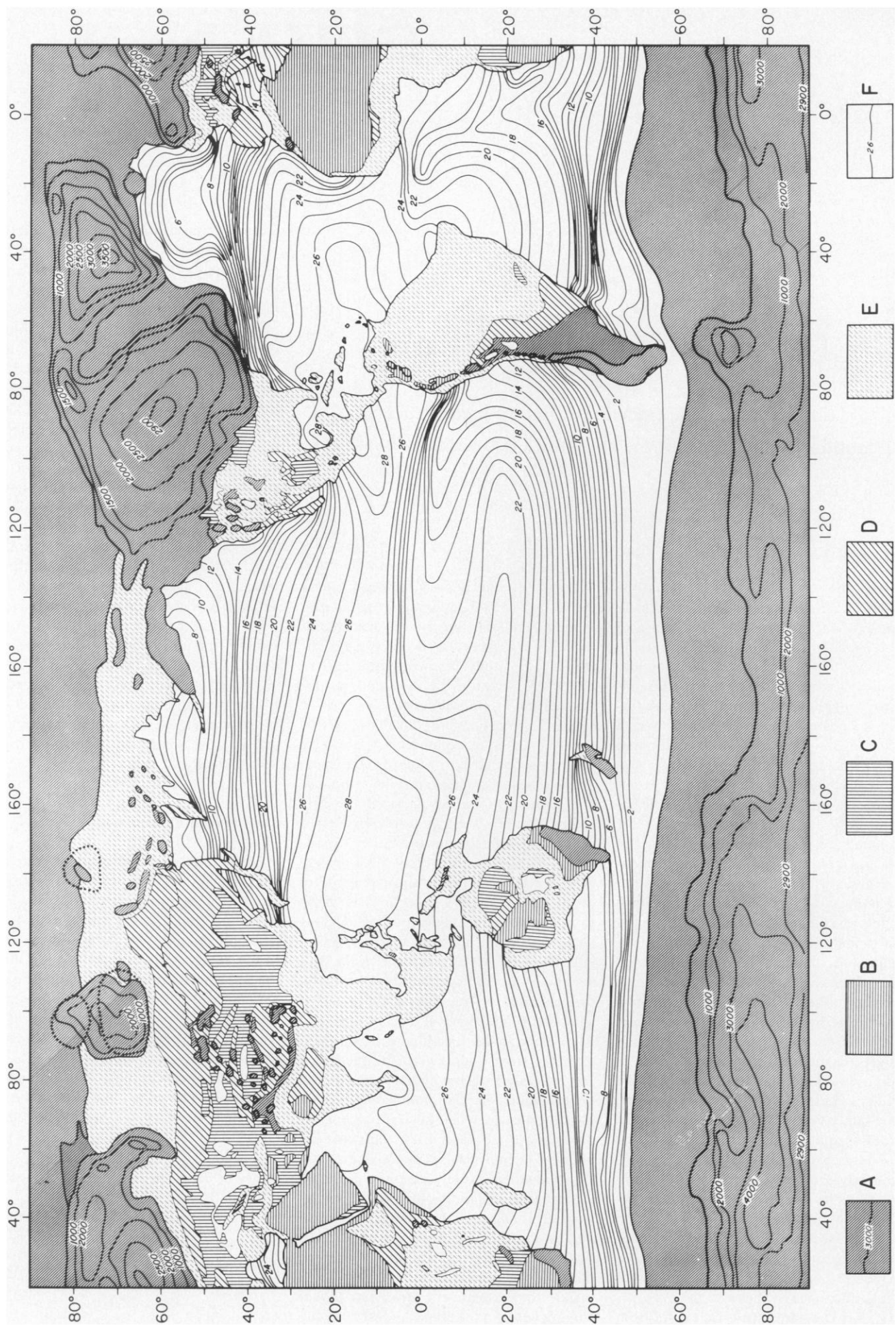
lations made with the current generation of GCM's, in which grid spacing ranges from approximately 250 to 500 km.

Land albedo. The first step in estimating the ground albedo of nonglaciated areas was to determine the distribution of vegetation and soil types in the glacial world. This determination was based on pollen, snow line, and various sedimentary-periglacial records. Except for Europe (*12, 13*) the data base was sparse and often poorly dated. The second step was to characterize the main types of surface cover by albedo estimates in the wavelength range 0.3 to 2.5 μm. These values were taken from published measurements of analogous modern ground (*14*). Although the reconstruction has a large margin of uncertainty, the effect of land-albedo errors on the GCM simulation is small compared to the thermal effect of sea and ice surfaces.

Ice sheets. The extent of ice sheets shown in Fig. 1 was derived from a survey of a large number of literature sources (*15–17*) supplemented by fieldwork (*18*). Several regions of the map are controversial; these are (i) the contact between the Cordilleran and Laurentide ice sheets (*19*); (ii) the position of the southern margin of the Cordilleran Ice Sheet (*20*); (iii) the extent of ice over the Queen Elizabeth Islands in northern Canada (*21*); (iv) the position of the ice margin on Baffin Island (*22*); (v) the extent of ice shelves in the Arctic (*23*); (vi) the extent of grounded ice in the Barents Sea (*24*); and (vii) the extent of the Antarctic Ice Sheet (*25–27*).

The ice margins derived for 18,000 B.P. were used as a base to reconstruct the large ice sheets in three dimensions. Equations from Paterson (*28*) yielded a series of profiles along flow lines. Altitudes given by these flow lines allowed contours to be

Fig. 1. Sea-surface temperatures, ice extent, ice elevation, and continental albedo for Northern Hemisphere summer (August) 18,000 years ago. Contour intervals are 1°C for isotherms and 500 m for ice elevation. Continental outlines represent a sea-level lowering of 85 m. In northern Siberia, dotted lines indicate a recently revised estimate of the ice extent; solid lines indicate the ice extent used in this experiment. To aid in the visualization of the thermal gradient along the North Atlantic Polar Front, alternate contour lines have been omitted in the western Atlantic. Albedo values are given by the key. (A) Snow and ice; albedo over 40 percent. Isolines show elevation of the ice sheet above sea level in meters. (B) Sandy deserts, patchy snow, and snow-covered dense coniferous forests; albedo between 30 and 39 percent. (C) Loess, steppes, and semideserts; albedo between 25 and 29 percent. (D) Savannas and dry grasslands; albedo between 20 and 24 percent. (E) Forested and thickly vegetated land; albedo below 20 percent (mostly 15 to 18 percent). (F) Ice-free ocean and lakes, with isolines of sea-surface temperature in degrees Celsius; albedo below 10 percent.

Table 1. Assemblages of planktonic microfossils and regression equations used to estimate sea-surface temperature. In the equation number code the first letter indicates the organism (F, foraminifera; C, coccoliths; R, radiolaria), the second letter the ocean (P, Pacific; I, Indian; S, Southern; and so forth), and the number the equation used. Values in the last column have been adjusted for degrees of freedom lost.

Equation number	Area	Species (N)	Assemblages (N)	Sum of squares accounted for by assemblages (%)	Standard error of estimate (°C)
FP1	Tropical Pacific	14	6	96	1.24
FP2	South Pacific	23	4	96	1.90
CP1	Pacific	16	6	98	1.42
RP1	North Pacific	44	4	92	0.92
RP2	Northeast Pacific	46	3	90	1.27
RP3	Temperate Pacific	46	4	91	2.69
RP4	West Pacific	48	3	92	1.02
RP5	North tropical Pacific	44	5	91	2.46
RP6	South tropical Pacific	51	4	96	1.98
FM1	Mediterranean	22	4	94	1.38
FI1	Indian	29	5	97	1.50
RS1	Antarctic	18	3	95	1.40
FA13	North Atlantic	29	6	92	1.38
FA14	South Atlantic	29	6	90	1.39

drawn for the upper surfaces of the large ice sheets (*29*). These techniques of ice-sheet reconstruction are only approximate because they involve simplifying assumptions concerned with the noncircular shape of the ice sheets, the temperature of basal ice, and the placement of ice-sheet domes.

Albedo values for the surface of the ice sheets in August were determined by calculating snow lines for large Northern Hemisphere ice sheets (*30*) and then assigning albedo values (*26–31*) for the several types of snow and ice surfaces in the accumulation and ablation areas. In higher latitudes of the Southern Hemisphere snow was assumed to cover glaciers in August.

The 18,000 B.P. Sea Surface

Paleoclimatic techniques. Recent developments in two paleoclimatic methods— biological transfer functions and oxygen isotope stratigraphy—make it possible to compile global charts of sea-surface temperature for the late Quaternary ocean. The transfer function method (*32–34*) provides a means of translating numerical descriptions of the planktonic biota preserved in deep-sea sediments into estimates of past seasonal sea-surface temperature. This technique uses a form of factor analysis that provides a number of empirical orthogonal functions to define biotic assemblages entombed on the modern seabed. These assemblages, which reflect the distribution of surface water masses, are then related to seasonal temperatures by multivariate regression equations. As shown in Table 1, three planktonic groups (Foraminifera, Radiolaria, and Coccolithophoridae) were used for both surface water-

mass delineation and temperature estimation in constructing the sea-surface temperature map (Fig. 1). The average standard error of estimate for individual samples is ± 1.6°C. Where isotherms on Fig. 1 are controlled by a set of N sample points (Fig. 2), the confidence interval is reduced by a factor of $N^{1/2}$.

Foraminifera alone were used for temperature estimation in the North Atlantic, Gulf of Mexico, Mediterranean Sea, Indian Ocean, and South Atlantic. Radiolaria were the main source of data for the Antarctic, with some overlap in coverage with Foraminifera in the South Atlantic and the Indian Ocean. In the Pacific all three groups were utilized. For samples on which more than one equation was used, agreement is nearly always within the standard errors of the equations (often within a fraction of 1°). Where differences exist between the various estimates, the coccolith equation was preferred because phytoplankton must be restricted to the near-surface waters of the euphotic zone. Significant disagreements (≥ 1.6°C) between the zooplankton and phytoplankton temperature estimates are limited to samples from the eastern equatorial Pacific region.

The extent of sea ice in the North Atlantic (*35*) and the Antarctic (*36*) was estimated from a combination of biologic and lithologic evidence. For example, cores between the Antarctic Polar Front and 65°S are characterized by highly diatomaceous sediments during interglacial and by clays during glacial ages. We infer that clay deposition indicates inhibition of diatom growth by permanent sea-ice cover. Thus, the northern limit of summer sea ice 18,000 B.P. was estimated by mapping the
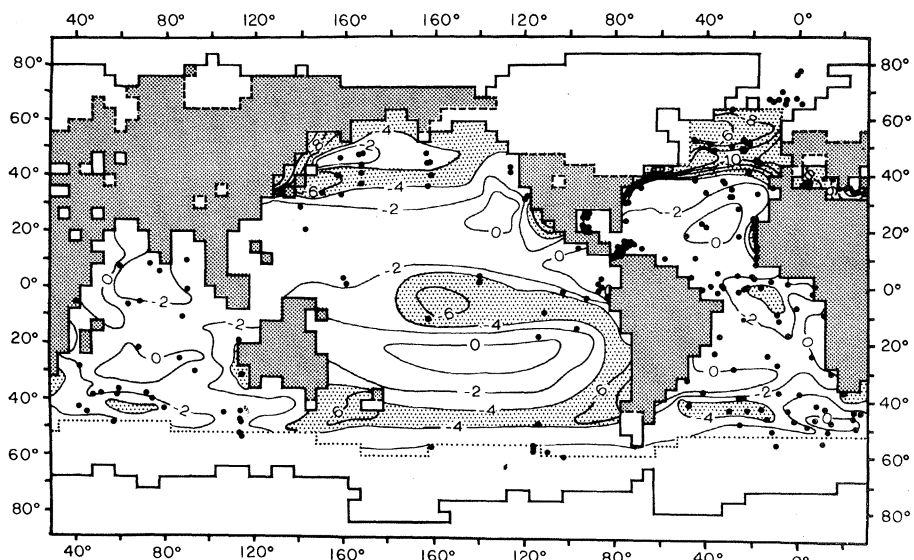
Fig. 2. Difference between August sea-surface temperatures 18,000 years ago and modern values. Contour interval is 2°C. Areas where the temperature change was greater than 4°C are shown in light stippling. Ice-free land areas are shown in darker stippling. Continental and ice outlines conform to a grid spacing of 4° latitude by 5° longitude. Heavy solid lines indicate continental outlines; dashed lines are ice margins on land; dotted lines indicate sea-ice margins. Large dots mark the locations of cores used in reconstructing sea-surface temperatures 18,000 years ago (38).

cores that show this distinctive lithologic sequence of glacial clay overlain by Holocene diatoms. The northern limit of winter (Southern Hemisphere) sea ice 18,000 B.P. must fall between the Antarctic Polar Front (identified faunally) and the summer ice boundary. We drew it halfway between.

The technique of isotopic stratigraphy is based on the demonstration that downcore variations in the oxygen isotope composition of calcareous shells reflect primarily variations in continental ice volume (37). Because these variations are synchronous within the mixing time of the world ocean, and have been dated in suitable cores by carbon-14, a detailed chronostratigraphic framework of global extent can be constructed. This framework, extended locally by standard micropaleontological and lithologic techniques, and checked againt carbon-14 dates, has made it possible to identify a set of 247 samples representing sediment that accumulated on the sea floor approximately 18,000 B.P. (38). The error in the selection of the 18,000 B.P. level is estimated to be less than ± 2000 years in most cores. If the marine climate was changing rapidly during the interval around 18,000 B.P., there might be serious inaccuracies in Fig. 1. However, there is ample evidence from deep-sea cores that the interval in question was relatively stable over the period from 24,000 to 14,000 B.P. (33).

Map construction. The process of constructing a paleoisotherm map (Fig. 1) is comprised of seven steps. First, a suite of deep-sea cores is obtained to provide both surface and downcore samples over a broad geographic area. Second, the relative abundance of the species in the surface

samples is determined, and species assemblages are defined by factor analysis (34). This provides a quantitative statement of the relative importance of each species in each assemblage and of each assemblage in each surface sample. The assemblages are then checked to see that they form coherent distributional patterns that can be related to surface water masses in the modern ocean (39–41). The third step is to establish, by means of a regression equation, the relationship between the average August sea-surface temperature (42) and the numerical value of the assemblages at each sample site (Table 2). This equation expresses sea-surface temperature as a function of the various assemblages (32). If the seabed data set includes a wide range of ecologic and diagenetic conditions, the equation is insensitive to nonthermal effects. The accuracy and reproducibility of the equations are then tested on an independent set of data (39). Fourth, the stratigraphy of the time interval under study is determined by using paleontological, geochemical, and paleomagnetic techniques, and a suite of isochronous samples are chosen that represent the sediment deposited at the time we wish to reconstruct. Each sample represents 1 cm of sediment and integrates the climatic record over a certain time interval. This interval is based on the average accumulation rate in our open-ocean cores (about 1 to 10 cm per 1000 years) and, allowing for mixing by burrowing organisms, it is estimated to range between 4000 and 400 years. Fifth, the microfossils in these sediments are examined and counted. Each sample is then described in terms of the assemblages de-

fined in the surface sediments. Sixth, from this numerical description of the ice-age samples in terms of modern assemblages, and the regression equations relating modern assemblages to temperature, an estimate of the 18,000 B.P. temperature is made for each sample. Finally, the results are plotted and contoured to yield paleoisotherm maps.

The reconstruction of sea-surface conditions (Fig. 1) was controlled by 247 data points. The quality of this control (Fig. 2) ranged from good in the North Atlantic to poor in the South Pacific. To guide the contouring in poorly controlled regions, therefore, it was helpful to formulate a general view of the nature of oceanic circulation at 18,000 B.P. and to employ biotic assemblages as water-mass indicators. Without exception, these radiolarian, foraminiferal, and coccolith assemblages are related to water-mass boundaries (39–41). It was therefore reasonable to assume that their distribution in the past can be used to indicate the positions of surface watermasses and currents. In the regions of poor control we assumed that changes in oceanic gyre geometry between 18,000 B.P. and today were similar to those that occurred in regions where our control is good—that is, that the major gyres of the ocean circulation were not disrupted at 18,000 B.P., but were shifted in position or changed in size or shape.

Discussion

Land albedo. The reconstruction of the distributions of vegetation types during the last ice age (Fig. 1) indicates that desert regions, steppes, grasslands, and outwash plains expanded at the expense of forests, yielding a slight increase in the albedo of land areas not covered by ice. Although the effect of this vegetational change on the dynamics of the global climate system may have been slight, the effect of the increase in albedo associated with the great expanse of land ice may have been quite large.

Cryosphere. The most striking feature of the 18,000 B.P. world was the Northern Hemisphere ice complex, consisting of land-based glaciers, marine-based ice sheets, and either permanent pack ice or shelf ice (Fig. 1). This complex stretched across North America, the polar seas, and parts of northern Eurasia. By contrast, large arctic areas in Alaska and Siberia remained unglaciated. In the Southern Hemisphere the most striking difference was the winter extent of sea ice, which was significantly greater than it is today. Changes in land ice were small. This extensive ice cover in the North Atlantic and southern oceans may have reduced the loss

1134

of heat from the oceans to the atmosphere in high latitudes (43), where today most of the world ocean's bottom and intermediate waters are formed. Permanent sea-ice cover in the Norwegian, Greenland, and Labrador seas must have precluded the formation of North Atlantic deep water.

The high-latitude ocean. In the North Atlantic the Gulf Stream shifted slightly southward off the Carolinas and swept almost directly eastward across the basin to the Iberian Peninsula (Fig. 1). The steep thermal gradient forming its northern boundary at 42°N marked the southern edge of the polar water mass. There was no strong northward transport of warm, higher-salinity waters such as occurs in the present North Atlantic Drift, Norwegian, and Irminger currents (44). The resulting temperature anomaly (Fig. 2) is seen as a belt of maximum values running from approximately 40°N in the west (−18°C maximum) to 50°N in the east (−12°C maximum). This area of pronounced change extended southward along Spain and included the northwest Mediterranean. The eastern Mediterranean, however, experienced a temperature decrease of only 1° to 2°C. Thus, whereas the temperature difference between the Balearic Islands and Crete is only 1° to 2°C today, the corresponding east-west gradient during the ice age was 10°C.

In the North Pacific there was a slight southward shift and steepening of the temperature gradient in the region between the Kuroshio and Oyashio currents. The resulting large negative temperature anomaly (−6° to −10°C) probably extended into the Sea of Japan (13, 45). Lowered sea level blocked the southern passage into this inland sea and prevented the northward flow of warm tropical waters. Similarly, lowered sea level completely blocked any incursion of Arctic waters into the Bering Sea. The amount of cooling in this area was small compared to that in equivalent latitudes in the North Atlantic (46).

Major differences between the Antarctic Ocean of 18,000 B.P. and that of today were the increase in thermal gradient and the northward movement of the polar front. In the Pacific this front shifted at least 4° of latitude (16, 47), in the western South Atlantic about 6°, and in the western Indian Ocean about 3°. Our data indicate little or no latitudinal displacement of the Subtropical Convergence; thus, the northward displacement of the Antarctic Polar Front resulted in an areal reduction of subantarctic water. Little or no temperature change occurred in the region between Africa and Antarctica, where flow is constrained by the boundaries of the basin.

The mid-latitude ocean. In mid-latitudes, the central gyres showed little, if

Table 2. Geographic distribution of the August ice-age sea-surface temperature anomaly, ΔT (°C). Values are averages weighted by area, excluding regions covered by sea ice.

| Area	ΔT (°C)
Northern Hemisphere	
Atlantic	−3.8
Pacific	−2.3
Indian	−0.8
Average	−2.6
Southern Hemisphere	
Atlantic	−1.7
Pacific	−2.6
Indian	−1.3
Average	−2.0
Global Ocean	−2.3

any, temperature change. In the Atlantic, Pacific, and southern Indian oceans, the polar fronts moved to lower latitudes and the subpolar and transitional water masses were reduced. Evidence for increased surface water transport in the eastern boundary currents of the North Atlantic is seen in the high gradients associated with the distribution of planktonic assemblages and with the derived thermal patterns. Along the west coast of North Africa, the southward deflection of isotherms probably reflects both the advection of cooler water and increased upwelling (48). On the western side of the basin, warm water moved north along the coast, but was deflected sharply eastward off Cape Hatteras. Tropical species, carried by this western boundary current, were found farther east at 18,000 B.P. than today. In the South Atlantic, northward flow of colder water in the glacial Benguela Current was greater than it is in the modern austral winter. The axis of the cold Benguela lobe (Fig. 1) appears to have been displaced westward and detached from the African coast; however,

the details of this pattern may be an artifact of the core coverage. Today the center of the thermal pattern that marks the Benguela flow extends to 10°E longitude at 20°S latitude and to 15°W longitude at the equator. Additonal cores now under study from the west African coast may alter this geometry by widening the thermal plume to the east, but the western boundary is well controlled. To the south, a small area with a negative temperature anomaly of up to −4°C appears off the tip of South Africa. This may reflect a decrease in the influence of the Agulhas Current at 18,000 B.P.

Negative anomaly patterns in the Indian Ocean differ from those in other oceans in that they tend to be meridional and to occupy both the eastern and western margins of the basin. The larger eastern anomaly is the result of increased equatorward flow of cool water along the coast of Australia, while the western anomaly is due to the absence of a strong Mozambique Current 18,000 B.P. We suggest that the Agulhas Current may not have been the major feature of the circulation that it is today and that the Mozambique Current turned east to parallel the West Wind Drift instead of joining the Agulhas Current. If this interpretation is correct, a strong anticlockwise gyre would have formed at temperate latitudes. Without a southern outlet for the advective loss of warm tropical waters, the regions may have become more thermally isolated.

In the eastern North Pacific, radiolarian species now found in the cool waters off Washington, Oregon, and northernmost California (41, 49) extended their distribution at least 1000 km to the south in the California Current. The southward shift of the frontal region associated with the California and North Equatorial currents re-

Fig. 3. Average sea-surface temperature difference between a modern August and August 18,000 B.P. (Solid line) Averages calculated by subtracting 18,000 B.P. temperatures (Fig. 1) from modern values (42) at each oceanic grid point not covered by sea ice, summing for each latitudinal band, and dividing by the number of grid points used. Grid spacing is 4° latitude by 5° longitude. (Dotted line) Average temperature differences weighted by the area of ice-free ocean along latitude bands 4° wide.
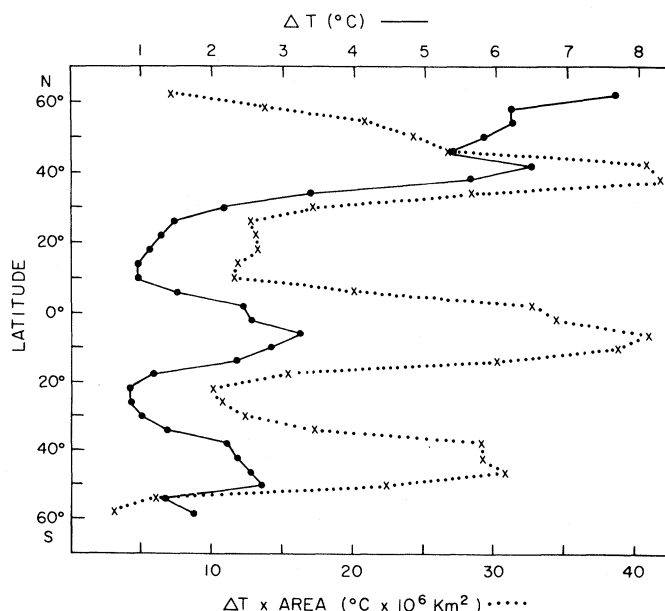
sulted in a large temperature decrease off the coast of northern Mexico (Fig. 2). The pool of warm water associated with the eastern end of the North Equatorial Countercurrent was shifted slightly to the south and extended into the Panama Basin, but there was little change in temperature. In the South Pacific the steepening of the temperature gradient in the subantarctic region probably gave rise to increased transport and cooler waters extending into the area of the Chile Current.

The low-latitude ocean. In the equatorial regions of the Pacific and Atlantic, a marked cooling is present at 18,000 B.P. This feature may have had as important an effect on climate as the equatorward displacement of polar fronts in the high-latitude oceans. Apparently, increased upwelling along the Pacific equatorial divergence produced temperatures that were as much as 6° cooler than today's. The present thermocline is very shallow in this region, and it is here that there is disagreement between the estimate of sea-surface temperature at 18,000 B.P. based on coccoliths and that based on radiolaria and foraminifera. This discrepancy suggests that the shallow thermocline broke down during the glacial interval, resulting in upwelling of cool waters to the surface. Such a change would have a pronounced effect on the habitats of the phytoplankton, but would appear as only a minor temperature change to the deeper-living zooplankton. Although the westward limit of this effect is not well known, the cool waters did not reach the western Pacific. Here, glacial temperatures were little different from those of today.

Similarly, in the Gulf of Mexico, Caribbean Sea, and western equatorial Atlantic, changes in surface temperature were less than 2°C (*48*). In the eastern equatorial region of the Atlantic, however, increased flow of the Benguela Current and upwelling along the divergence apparently lowered surface water temperatures by approximately 5°C (*35*). This general cooling of equatorial waters was not pronounced in the Indian Ocean. Except for cooler water in the eastern Arabian Sea, which may indicate increased upwelling, there was little change in sea-surface temperatures. Like the anomaly in the eastern Mediterranean, changes over the low-latitude Indian Ocean do not exceed 2°C.

The world ocean. Perhaps the most important conclusion to be drawn from Fig. 2 is that the ice-age surface-temperature change was not, in general, very large; the average anomaly over the entire ocean is only −2.3°C (Table 2). In the Northern (summer) Hemisphere the large shift in the path of Gulf Stream waters causes the Atlantic to have the highest anomaly. In

the Southern (winter) Hemisphere the marked cooling along the South Equatorial Current gives the Pacific the largest average difference in temperature. Additional insights into the spatial pattern of climate change can be gained from a latitudinal plot of zonally averaged sea-surface temperature anomalies (Fig. 3). On this plot, the changes at high northern latitudes appear to dominate the pattern. If this curve is weighted according to the area of ice-free ocean along discrete latitudinal bands, then the maximum effects occur at about 38°N, 6°S, and 46°S and are roughly of the same magnitude.

The increase in divergence and the compression of thermal gradients, indicated by these maximums and seen in Figs. 1 and 2, suggest a more energetic circulation system. Certainly surface transport was increased, and probably a more rapid turnover of surface and intermediate waters was effected. Inferences about the structure of deeper waters are more tenuous. However, previous studies of deep-sea benthonic foraminifera have indicated that changes in the distribution of deep-water masses of the North Atlantic did occur during the last glacial maximum (*50*). These findings, combined with our evidence that near-surface waters were cooler and better mixed and with our inference that a greater conservation of heat occurred beneath sea ice at high latitudes, suggest that the thermal contrast between surface and bottom waters of the 18,000 B.P. ocean was less than it is today.

Summary

In the Northern Hemisphere the 18,000 B.P. world differed strikingly from the present in the huge land-based ice sheets, reaching approximately 3 km in thickness, and in a dramatic increase in the extent of pack ice and marine-based ice sheets. In the Southern Hemisphere the most striking contrast was the greater extent of sea ice. On land, grasslands, steppes, and deserts spread at the expense of forests. This change in vegetation, together with extensive areas of permanent ice and sandy outwash plains, caused an increase in global surface albedo over modern values. Sea level was lower by at least 85 m.

The 18,000 B.P. oceans were characterized by: (i) marked steepening of thermal gradients along polar frontal systems, particularly in the North Atlantic and Antarctic; (ii) an equatorward displacement of polar frontal systems; (iii) general cooling of most surface waters, with a global average of −2.3°C; (iv) increased cooling and upwelling along equatorial divergences in the Pacific and Atlantic; (v) low temperatures

extending equatorward along the western coast of Africa, Australia, and South America, indicating increased upwelling and advection of cool waters; and (vi) nearly stable positions and temperatures of the central gyres in the subtropical Atlantic, Pacific, and Indian oceans.

References and Notes

1. U.S. Committee for the Global Atmospheric Research Program, National Research Council, *Understanding Climatic Change, A Program For Action* (National Academy of Sciences, Washington, D.C., 1975).
2. J. Smagorinsky, in *Weather And Climate Modification*, W. N. Hess, Ed. (Wiley, New York, in press); R. G. Barry, *Palaeogeogr. Palaeoclimatol. Palaeoecol.* **17**, 123 (1975).
3. W. L. Gates, *Science* **191**, 1138 (1976); _____, E. S. Batten, A. B. Kahle, A. B. Nelson, *A Documentation of the Mintz-Arakawa Two-Level Atmospheric General Circulation Model* (R-877, Rand Corporation, Santa Monica, Calif., 1971); W. L. Gates, *J. Atmos. Sci.* **32**, 449 (1975).
4. Lamont-Doherty Geological Observatory of Columbia University, Brown University, Case Western Reserve University, Oregon State University, University of Maine, University of Rhode Island, Queens College of the City University of New York, University of Wisconsin, University of Southern California, University of Arizona, University of Cincinnati, Rand Corporation, U.S. Naval Oceanographic Office, Cambridge University, University of Bergen, University of Kiel, University of Amsterdam, University of East Anglia, and University of Copenhagen,
5. CLIMAP is an acronym for Climate: Long-Range Investigation Mapping and Prediction.
6. J. Williams, R. G. Barry, W. M. Washington, *J. Appl. Meteorol.* **13**, 305 (1974).
7. J. L. Holloway, Jr., and S. Manabe, *Mon. Weather Rev.* **99**, 335 (1971).
8. The task groups responsible for gathering data used in the global reconstruction of the earth 18,000 B.P. are as follows (group leaders' names are given in italics): Compilation: *A. McIntyre* and T. Moore. Coordinator: *J. Imbrie.* Sea level: *R. Matthews* and S. Mangion. Ice: *G. Denton*, B. Andersen, and P. Mayewski. Albedo: *G. Kukla* and H. Kukla. Isotope stratigraphy: *N. Shackleton.* Sea surface: (North Atlantic) *A. McIntyre*, N. Kipp, W. Ruddiman, T. Kellogg, W. Prell, J. Gardner, T. Crowley, and A. Bé; (Gulf of Mexico) *J. Kennett*, C. Brunner, and J. Cooley; (Mediterranean) *J. Imbrie*; (South Atlantic) *N. Kipp*, B. Molfino, W. Balsam, H. Thierstein, and J. Gardner; (Antarctic) *J. Hays*, J. Lozano, and G. Irving; (Indian Ocean) *A. Bé*, T. Kellogg, and W. Hutson; (Pacific) *T. Moore*, H. Sachs, J. Robertson, T. Saito, P. Thompson, K. Geitzenauer, B. Luz, N. Opdyke, and D. Ninkovich.
9. J. R. Curray, in *The Quaternary of the United States*, H. E. Wright and D. G. Frey, Eds. (Princeton Univ. Press, Princeton, N.J., 1965), pp. 723–735; A. L. Bloom, in *The Late Cenozoic Glacial Ages*, K. K. Turekian, Ed. (Yale Univ. Press, New Haven, Conn., 1971), pp. 355–379.
10. Some dated materials are unquestionable indicators of past sea level, whereas others, such as some species of mollusks and corals, could have lived as much as 75 to 100 m below sea level. We choose to view the data with caution. The oyster *Crassostrea virginica*, however, is an excellent indicator of low-salinity, nearshore waters. The lowest sea-level estimate yielded by samples containing this species is −90 m at 17,000 years ago [J. R. Curray, in *Recent Sediments, Northwest Gulf of Mexico*, F. P. Shepard, F. B. Phleger, T. H. van Andel, Eds. (American Association of Petroleum Geologists, Tulsa, Okla., 1960), p. 221].
11. Recent developments concerning the viscosity of the mantle [L. M. Cathles, III, thesis, Princeton University (1971); R. I. Walcott, *Quat. Res.* **2**, 1 (1972)] suggest that data from continental margins contain a combination of eustatic and isostatic information. A. L. Bloom [*Geol. Soc. Am. Bull.* **78**, 1477 (1967); *Quaternaria* **12**, 145 (1970)] has suggested that oceanic islands should provide a true record of sea-level history, independent of the viscous response of the mantle to changing loads.
12. B. Frenzel, *Abh. Math. Naturwiss. Kl. Akad. Wiss. Lit.* **6**, 290 (1960).
13. _____, *Science* **161**, 637 (1968).
14. V. Mukhenberg, *Trans. Main Geophys. Obs. Leningrad* **139**, 43 (1963); J. W. Posey and P. F. Clapp, *Geofis. Int.* **4** (No. 1), 53 (1964); D. B. Miller and R. G. Feddes, *Eos* **52**, 228 (1971).
15. R. F. Flint, *Glacial and Quaternary Geology* (Wiley, New York, 1971), p. 892.

16. ———, *Glacial and Pleistocene Geology* (Wiley, New York, 1957), p. 553.

17. V. K. Prest, *Retreat of Wisconsin and Recent Ice in North America* (Map 1257A, Geological Survey of Canada, Ottawa, 1969).

18. For this first experiment, the accuracy for the placement of the ice margin needed only to fit within the computer grid spacing of 4° latitude by 5° longitude; however, every effort was made to bring the accuracy to within a 1° by 1° framework.

19. The nature of the contact between the Cordilleran and Laurentide ice sheets of North America is not entirely clear. Although some authors (*17*) indicate that the two sheets may have coalesced, others [B. O. K. Reeves, *Arct. Alp. Res.* 5 (No. 1), 1 (1973)] claim that there is no incontrovertible evidence for such coalescence in the late part of the last glacial. In Fig. 1 we have followed the current opinion of workers (J. A. Westgate and N. W. Rutter, personal communication) in the region and left only the southern portion of the contact area open.

20. Radiocarbon dates from southern British Columbia and northern Washington State indicate that the southern margin of the Cordilleran Ice Sheet was somewhat retracted about 18,000 B.P. and did not attain its maximum Late Wisconsin position until about 14,000 B.P. [S. C. Porter, in *The Late Cenozoic Glacial Ages*, K. K. Turekian, Ed. (Yale Univ. Press, New Haven, Conn., 1971), pp. 307–329]. Accordingly, this margin is drawn behind its maximum position (R. J. Fulton, personal communication).

21. The extent of ice over the Queen Elizabeth Islands in northern Canada is under discussion. Figure 1 follows Blake [W. Blake, Jr., *Can. J. Earth Sci.* 11, 1025 (1974); *ibid.* 7, 634 (1970)] and shows an extensive Innuitian Ice Sheet that abuts both the Laurentide and Greenland sheets. However, the alternative argument of limited ice cover over these islands reaching a Late Wisconsin (most recent glacial interval) maximum about 8100 B.P. may well be viable [J. H. England, thesis, University of Colorado, Boulder (1974)].

22. It has been suggested that the extensive Cockburn moraine system, which has been dated at only 8000 to 8200 B.P. and which trends along the east coast of Baffin Island, represents the maximum extent of Late Wisconsin Laurentide ice [J. T. Andrews, A. Means, G. H. Miller, *Nature (London)* 239, 147 (1972)]. If so, it is difficult to delineate the ice margin at 18,000 B.P. Thus, we have followed Andrews (J. T. Andrews, personal communication) and placed the 18,000 B.P. margin at the Cockburn moraine system.

23. Ice shelves may have been widespread in the Arctic [J. H. Mercer, *Palaeogeogr. Palaeoclimatol. Palaeoecol.* 8, 19 (1970); W. S. Broecker, *Science* 188, 1116 (1975)]. In fact, thick ice shelves may well have covered the Arctic Ocean, the Greenland and Norwegian seas, and the Baffin Bay–Davis Strait–Labrador Sea region. However, they are left out in this initial synthesis because the difference between the shelf ice and permanent pack ice over polar seas is unimportant for this modeling experiment.

24. The existence of grounded ice in the Barents Sea during Late Wisconsin time has been demonstrated [V. Schytt, G. Hoppe, W. Blake, Jr., M. G. Grosswald, *Int. Assoc. Sci. Hydrol. Int. Union Geol. Geophys.* 79, 207 (1968); M. G. Grosswald, *Geology* 1, 77 (1972)]. However, the exact dimen-

sions of this sheet, as well as its relation to Scandinavian ice, are unclear. Hence, Fig. 1 represents the situation somewhat stylistically.

25. The extent of the Antarctic Ice Sheet at 18,000 B.P. is not well defined. We have expanded the East Antarctic sheet somewhat along the coast (*26, 27*) to compensate for adjustment to a lower Late Wisconsin sea level and, as is consistent with field evidence, have kept the interior surface altitude very close to present values. There is evidence that the ice sheet in West Antarctica, which is largely grounded below sea level, may have undergone considerable expansion into the Ross and Weddell seas during Late Wisconsin time. However, pending further investigation, a conservative view of such expansion is taken in Fig. 1.

26. C. R. Bentley *et al.*, *Physical Characteristics of the Antarctic Ice Sheet* (Antarctic Map Folio Series, Folio 2, American Geological Society, New York, 1964).

27. G. H. Denton, R. L. Armstrong, M. Stuiver, in *The Late Cenozoic Glacial Ages*, K. K. Turekian, Ed. (Yale Univ. Press, New Haven, Conn., 1971), pp. 267–306; P. A. Mayewski, *Institute of Polar Studies Report* (Ohio State University, Columbus, in press).

28. W. S. B. Paterson, *Rev. Geophys. Space Phys.* 10, 885 (1972).

29. The maximum ice-surface altitude for the Laurentide Ice Sheet is given as 2900 m; this is 200 m higher than Paterson's value (*28*) because we estimated the average altitude of northern and northeastern North America at 200 m rather than at sea level.

30. J. Weertman, *J. Glaciol.* 6 (No. 44), 191 (1966); *J. Geophys. Res.* 66, 3783 (1961).

31. R. Geiger, *The Climate Near the Ground* (Harvard Univ. Press, Cambridge, Mass., 1966), p. 611.

32. J. Imbrie and N. Kipp, in *The Late Cenozoic Glacial Ages*, K. K. Turekian, Ed. (Yale Univ. Press, New Haven, Conn., 1971), p. 71; J. Imbrie, J. van Donk, N. G. Kipp, *Quat. Res.* 3, 10 (1973).

33. See figures A-11 and A-13 in (*1*).

34. In the form of analysis used (Q-mode factor analysis) eigenvectors from the major cross product of a row-normalized data matrix are calculated, and then an orthogonal, varimax rotation is performed [J. E. Klovan and J. Imbrie, *Math. Geol.* 3 (No. 1), 61 (1971)].

35. T. Kellogg, in *Climate of the Arctic*, G. Weller and S. A. Bolliny, Eds. (Geophysical Institute, University of Alaska, Fairbanks, 1975), p. 3; A. McIntyre *et al.*, *Geol. Soc. Am. Mem.* 145, in press.

36. J. D. Hays, J. Lozano, N. Shackleton, G. Irving, *Geol. Soc. Am. Mem.* 145, in press.

37. N. J. Shackleton and N. D. Opdyke, *Quat. Res.* 3, 39 (1973).

38. A data file of all cores used in the construction of the 18,000 B.P. sea-surface temperature map has been stored with the Marine Geological and Geophysics Branch, National Geophysics and Solar-Terrestrial Data Center, National Oceanic and Atmospheric Administration, Boulder, Colorado. This file contains core location, sample depth, estimated age error, and estimated temperature.

39. N. Kipp, *Geol. Soc. Am. Mem.* 145, in press.

40. J. Lozano and J. D. Hays, *ibid.*, in press; K. Geitzenauer, *ibid.*, in press; H. M. Sachs, *Quat. Res.* 3, 73 (1973).

41. T. C. Moore, Jr., *Quat. Res.* 3, 99 (1973).

42. August sea-surface temperature data are from the

National Oceanographic Data Center, Washington, D.C., and from charts in the following publications: K. Wyrtki, *Oceanographic Atlas of the International Indian Ocean Expedition* (National Science Foundation, Washington, D.C., 1971); W. S. Wooster, *Scientific Exploration of the South Pacific* (National Academy of Sciences, Washington, D.C., 1970); *Oceanographic Atlas of the North Atlantic Ocean II* (Publ. 700, Naval Oceanographic Office, Washington, D.C., 1967); *Oceanographic Atlas of the Polar Seas. 1, Antarctic. II, Arctic* (Publ. 705, Naval Hydrographic Office, Washington, D.C., 1957, 1958); *Monthly Charts of Mean Minimum and Maximum Sea Surface Temperature of the North Pacific Ocean* (Spec. publ. 123, Naval Oceanographic Office, Washington, D.C., 1969); *World Atlas of Sea Surface Temperature* (Publ. 225, Naval Hydrographic Office, Washington, D.C., 1944; ed. 2, 1954).

43. R. Newell, *Quat. Res.* 4, 117 (1974).

44. P. K. Weyl, *Meteorol. Monogr.* 8, 37 (1968).

45. T. Kobayashi and T. Shikama, in *Descriptive Paleoclimatology*, A. E. M. Nairn, Ed. (Interscience, New York, 1961), p. 292.

46. P. Colinvaux, in *The Bering Land Bridge*, D. M. Hopkins, Ed. (Stanford Univ. Press, Stanford, Calif., 1967), p. 207.

47. In the South Pacific, control points are sparse for the 18,000 B.P. map. Data from studies of Pleistocene sediments on land indicate that glaciers in southern Chile reached the sea at sites as far north as 43°S and that temperatures in the southern part of central Chile were as much as 5°C cooler during the late-glacial growing season [C. A. Laugenie and J. H. Mercer, *Abstr. 9th Int. Conf. INQUA (Int. Quat. Assoc.)* (1973), p. 202; C. J. Heusser, *Proc. Am. Philos. Soc.* 110, 269 (1966); R. F. Flint, *Glacial and Pleistocene Geology* (Wiley, New York, 1957), pp. 680–715.

48. J. V. Gardner and J. D. Hays, *Geol. Soc. Am. Mem.* 145, in press; W. Prell, *ibid.*, in press.

49. C. A. Nigrini, *Geol. Soc. Am. Mem.* 126 (1970), p. 139.

50. S. S. Streeter, *Quat. Res.* 3, 131 (1973); D. Schnitker, *Nature (London)* 248, 385 (1974).

51. Supported by NSF grants IDO 71-04204 to Lamont-Doherty Geological Observatory of Columbia University (LDGO), GX 28672 to Brown University, GX 28673 to Oregon State University, and GX 39773 to the University of Maine. Other research that contributed to the study was supported by NSF grants DES 72-01667 A02 to J. Kennett and DES 73-00467-A01 to A. McIntyre and W. Ruddiman, ARPA grant F44620-73-C-0021 to J. Imbrie, and grant GR 3/1762 from the National Environmental Research Council (England) to N. J. Shackleton. This research would not have been possible without the large core collection of LDGO maintained under NSF grant DES 72-01568 and ONR N00014-75-C-0210. We also thank the core curators at Oregon State University, the University of Southern California, Scripps Institution of Oceanography, and Florida State University for their cooperation and aid in obtaining surface and downcore samples. All of our CLIMAP associates and cooperative researchers, who have willingly and freely discussed with us the many problems involved in the production of this work, are gratefully acknowledged. This article is Lamont-Doherty Geological Observatory Contribution 2314.